International Journal of Engineering Research-Online
A Peer Reviewed International Journal
Articles available online http://www.ijoer.in

Vol.3., S3, 2015

NCERFM-2015

ISSN: 2321-7758

# EFFECT OF ANNEALING TEMPERATURE ON THE MAGNETIZATION OF COBALT FERRITE

[1]G. H. KALE, [2]ASHOK V. HUMBE, [3]G. B. JADHAV, [4]P. K. GAIKWAD, [5]R. C. ALANGE, *[2]K. M. JADHAV

[1]Yashwantrao Chavan Mahavidyaly, Tuljapur, Osmanabad, Maharashtra, India
[2]Dr. Babasaheb Ambedkar Marathwada University, Aurangabad, Maharashtra, India
[3]B. S. S. Arts Science College, Makni, Osmanabad, Maharashtra, India
[4]S. C. S. College, Omerga, Osmanabad, Maharashtra, India
[5]Shri. Madhavrao Patil Mahavidyalay, Murum, Osmanabad, Maharashtra, India
*Corresponding author: drjadhavkm@gmail.com

**ABSTRACT**

The structural, morphological and magnetic properties of Cobalt ferrite nanoparticles as a function of annealing temperature have reported in the present work. Cobalt ferrite nanoparticles were prepared by sol-gel auto-combustion technique using high purity metal nitrates and L-Ascorbic acid as a fuel. The as prepared powder was annealed at temperatures $600^0C$, and $1000^0C$. The annealed powder was used for further characterization. The nanocrystalline form of prepared samples was confirmed by X-ray diffraction (XRD) as well as scanning electron microscopy (SEM). The structural parameters like lattice constant, X-ray density, crystallite size were obtained from XRD data. The grain size was obtained from SEM images. The magnetic properties were studied at room temperature using M-H hysteresis plots and effect of annealing temperature is presented. The M-H plots used to evaluate the values of saturation magnetization (Ms), remenance magnetization (Mr), magneton number and coercivity (Hc) for all samples. The magnetization analysis revealed that the saturation magnetization increases whereas coercivity and remanence magnetization decreases with increasing annealing temperature. The magneton number also increases with increasing temperature. The observed magnetic parameters of present $CoFe_2O_4$ samples are found to be better as compared to bulk $CoFe_2O_4$.

**Keywords:** Cobalt ferrite nanoparticles, sol-gel auto-combustion, annealing temperature, magnetic properties

## 1 INTRODUCTION

Nanocrystalline materials due to their interesting physical and chemical properties are of great importance in the recent years from the research and technological applications point of view [1, 2]. Nanocrystalline materials exhibit unique crystallo-graphical structure e.g., high surface area and high volume fraction of atoms at interfacial regions. The resulting properties namely super-paramagnetism, super-plasticity, catalytic activity etc are distinctly different from those of their micrometer sized counterparts [3]. The physical and chemical properties are greatly influenced by the synthesis root and various synthesis parameters.

Metal oxide nanoparticles in particular spinel ferrites are of current focus because of their interesting optical, electronic, mechanical, structural and magnetic properties and have large number of promising technological applications in high density recording media, ferrofluids, drug delivery, magnetic refrigerators, high frequency devices [4,5] etc.

In the family of spinel ferrite, cobalt ferrite ($CoFe_2O_4$) with inverse spinel structure has been widely studied [6, 7] as they display attractive magnetic properties as well as electrical and other properties making them useful in wide range of applications. Cobalt ferrite possess high Curie temperature, high magnetocrystalline anisotropy, high permeability, high coercivity, high saturation magnetization, good magnetic mechanical properties, excellent chemical stability etc and therefore is subject of interest of researchers. The compositional and micro-structural properties are sensitive to the preparation method used for their synthesis. The magnetic nanoparticles of cobalt ferrite can be obtained by variety of methods including sol-gel [8], hydrothermal [9], co-precipitation [10], microemulsion [11] etc. The magnetic nanoparticles with a higher surface area to volume ratio provide higher sensitivity, better targeting and improvement of the colloidal stability of the nanostructures [12].

Like synthesis methods, synthesis parameters and synthesis conditions also strongly influences the physical and chemical properties of spinel ferrite nanoparticles. In the literature, there are reports on the effect of fuel additives [13], chelating agent [14], and aging time [15] on structural, microstructural and magnetic properties of cobalt ferrite nanoparticles. The influence of heat treatment on cobalt ferrite ceramic powder was reported by Juliana B. Silva et.al [16]. To the best of our knowledge the effect of variation of annealing temperature on the structural, morphological and magnetic properties of cobalt ferrite nanoparticles is not systematically reported in the literature.

In the present investigation, cobalt ferrite nanoparticles were prepared by sol-gel auto-combustion method relatively at low temperature using L-Ascorbic acid as a fuel and maintaining metal nitrates to fuel ratio as 1:3. The prepared powder of cobalt ferrite was annealed at different temperatures viz 600°C and 1000°C to understand the effect of varying annealing temperature on the structural and magnetic properties of cobalt ferrite nanoparticles investigated by X-ray diffraction, scanning electron microscope. The magnetic properties were investigated through M-H hysteresis loop tracer technique method.

## 2 Materials and Methods

### *2.1 Preparation of cobalt ferrite nano-particles*

The nano-powders of cobalt ferrite were synthesized by well known sol-gel auto-combustion as described method [17] using metal nitrates of respective ions and L-Ascorbic acid, as a fuel. The obtained powder was annealed at $600^0$C and $1000^0$C and further used for characterizations. Cobalt ferrite nano-particles synthesized by sol-gel auto-combustion method at $600^0$C and $1000^0$C were named as CF6 ($CoFe_2O_4$ sintered at $600^0$C) and CF10 ($CoFe_2O_4$ sintered at $1000^0$C) respectively.

### *2.2 Characterizations*

The X-ray diffraction technique was employed to confirm the phase purity and nano crystalline nature of the prepared cobalt ferrite nano-particles. The X-ray diffraction pattern was recorded into 2θ range of $20^0$-$80^0$ at room temperature using Cu-Kα radiation. The surface morphological studies were carried out using scanning electron microscopy technique

The magnetic measurements were recorded at room temperature using pulse field hysteresis loop technique.

**Table 1:** Various parameters for cobalt ferrite nanoparticles as function of annealing temperature

| Sr. No. | Parameters | $CoFe_2O_4$ sintered at $600^0$C | $CoFe_2O_4$ sintered at $1000^0$C |
|---|---|---|---|
| 1 | Lattice constant (a) | 8.357 Å | 8.388 Å |
| 2 | X-ray density ($d_x$), | 5.365 gm/cm$^3$ | 5.281 gm/cm$^3$ |
| 3 | Bulk density ($d_B$) | 3.561 gm/cm$^3$ | 3.773 gm/cm$^3$ |
| 4 | Porosity (P), | 34% | 29% |
| 5 | Crystallite size (t) | 33 nm | 48 nm |
| 6 | Saturation magnetization (Ms), | 80.21 emu/gm | 86.22 emu/gm |
| 7 | Remenance Magnetization (Mr), | 69.27 emu/gm | 66.22 emu/gm |
| 8 | Coercivity (Hc) | 2444 Oe | 998 Oe |
| 9 | Magneton number ($n_B$) | 3.37 | 3.62 |

## 3 Results and Discussion

### 3.1 X-Ray Diffraction

Figure 1(a, and c) represents the X-ray diffraction (XRD) pattern of cobalt ferrite samples annealed at temperatures $600^0$C and $1000^0$C namely CF6 and CF10 respectively. All the XRD patterns exhibit similar kind of nature except the peak intensity and broadening. The reflections present in the XRD pattern belongs to cubic spinel structure. The analysis of XRD pattern was made through computer program and it indicates that all the samples possess single phase cubic spinel structure with no extra peaks. A careful examination of the XRD pattern shows that the intensity of Bragg's reflection increases with increase in annealing temperature. Besides that the broadening of the most intense peak (311) of the XRD pattern slightly decreases with increasing annealing temperature. The increase in broadening, intensity and sharpness is attributed to increasing annealing temperature.

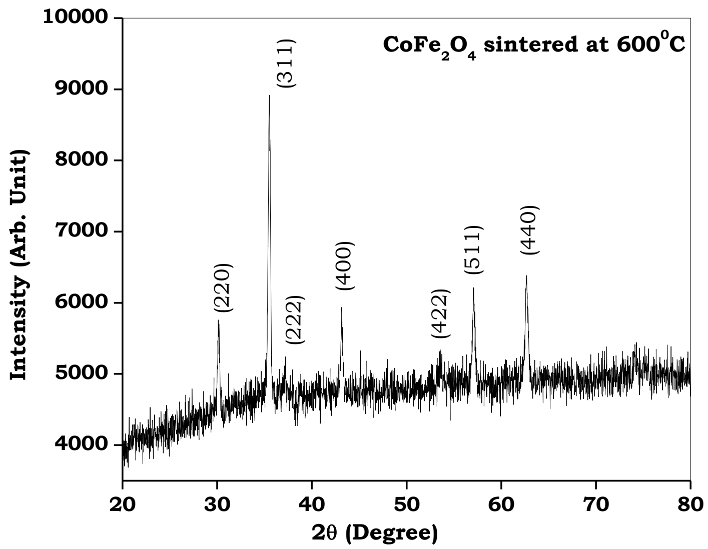


**Fig 1 (a):** XRD Pattern of cobalt ferrite nano-particles prepared by sol-gel auto-combustion method using L-Ascorbic Acid as a fuel sintered at 600$^0$C.

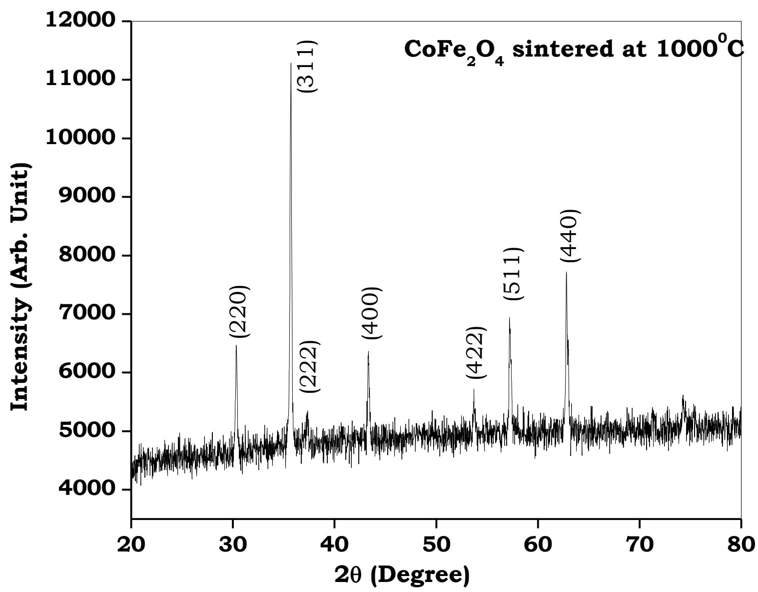


**Fig 1 (b):** XRD Pattern of cobalt ferrite nano-particles prepared by sol-gel auto-combustion method using L-Ascorbic Acid as a fuel sintered at 1000$^0$C.

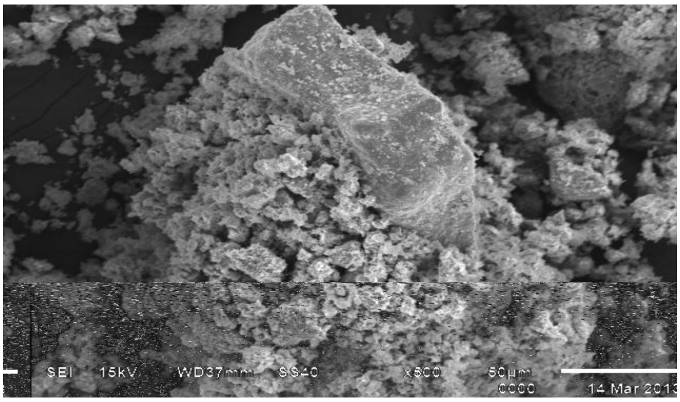


**Fig 2 (a):** Scanning electron micrograph (SEM) of cobalt ferrite nano-particles prepared by sol-gel auto-combustion method.

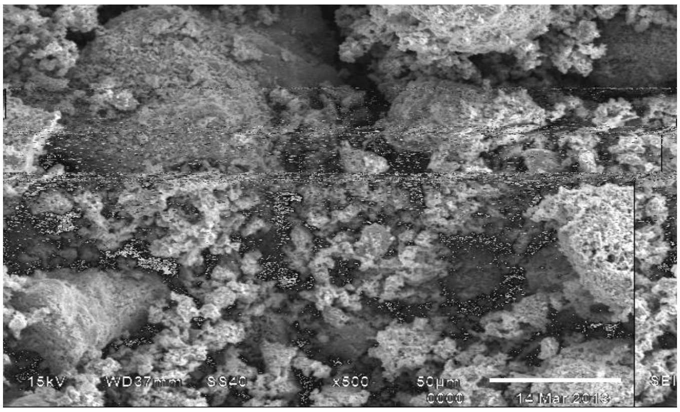


**Fig 2 (b):** Scanning electron micrograph (SEM) of cobalt ferrite nano-particles prepared by sol-gel auto-combustion method.

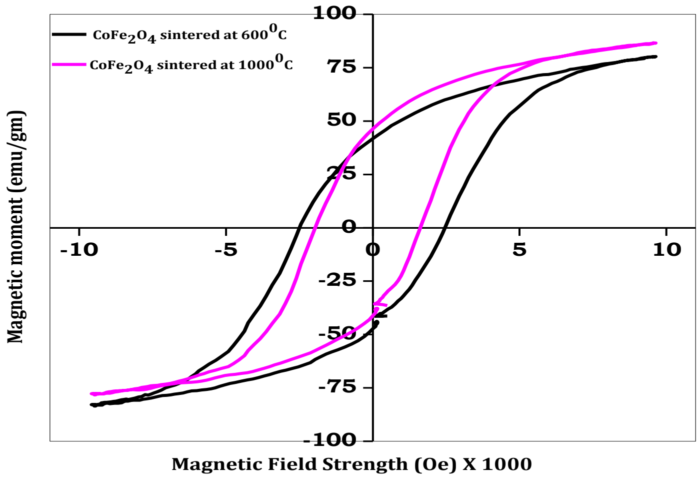


**Figure 3:** M-H plots of cobalt ferrite nano-particles prepared by sol-gel auto-combustion technique.

Using XRD data the lattice constant (a) was determined for both the samples (CF6 and CF10) using the standard relation for cubic symmetry given by

$$a = d\sqrt{N} \qquad \text{.................(1)}$$

where, notations have their usual meaning. The values of lattice constant are presented in Table 1. It can be observed from Table that, the lattice constant increases as annealing temperature increases. Similar behavior of lattice constant was reported in the literature [18].

The X-ray density $d_x$ was determined by using the following relation,

$$d_x = \frac{ZM}{NV} \quad \text{.................(2)}$$

where, Z = 8 for cubic spinel ferrite, M is molecular weight, N Avogadro's Number and V is volume of the unit cell.

The values of X-ray density are presented in Table 1. It is found from table that X-ray density decreases with increase in annealing temperature. The decrease in X-ray density is attributed to increasing unit cell volume due to increase in lattice constant.

The bulk density ($d_B$) was determined through Archimedes Principle and their values are reported in the Table 1. It is evident from table that bulk density decreases with increasing temperature. Due to increase in temperature lattice constant increases and hence unit cell volume also increases. The increase in volume overtakes increase in mass and hence bulk density decreases.

The porosity (P) of the samples was determined through the values of X-ray density and bulk density. Table 1 shows the values of percentage porosity for both the samples under investigation. The porosity decreases with increase in annealing temperature. The high porosity of 34% is observed for the sample CF6 may be due to more agglomeration. The low density of 29% is observed for the samples CF10 may be due to higher annealing temperature causing the reduction in number of pores.

The crystallite size (t) of all the samples was calculated using Scherer's formula [19], for which the most intense peak (311) was considered. The values of crystallite size are presented in Table 1. It is evident from Table 1 that the crystallite size increases as annealing temperature increases.

Thus, the increase in annealing temperature results in increase in crystallite size their by affecting the structural properties of the cobalt ferrite.

**3.2 Scanning Electron Microscope**

The microstructure and surface morphology of the present samples was studied using scanning electron microscopy (SEM) technique. Figure 2 (a and b) shows the SEM images of the samples CF6 and CF10 respectively. The analysis of SEM image shows that the microstructures of the cobalt nanoparticles were almost regular in shape and dispersed uniformly. The agglomeration of particles at 600 °C that is for sample CF6 is more as compared to CF10. Using the SEM image the grain size (G) was calculated using linear intercept method. Table 1 provides the values of grain size as a function of annealing temperature. It is observed from Table 2 that, the grain size of both the samples is in nanometer range and increases with increasing annealing temperature. Our results on scanning electron microscopy technique are in good agreement with the literature reports [20]. Thus, the nanocrystalline nature of the samples was confirmed through grain size values.

**3.3 Magnetic properties**

The magnetic properties tested by pulse field hysteresis loop tracer technique at room temperature for cobalt ferrite nanoparticles. The samples show strong influence of annealing temperature. The magnetization (M) versus applied magnetic field (H) that is M-H plots for both the samples are shown in Figure 3. The plot indicates the normal hysteresis loop and was used to evaluate the values of saturation magnetization (Ms), remenance magnetization (Mr) and coercivity (Hc). Table 1 illustrates the values of all these magnetic parameters for different annealing temperature. It can be noticed from Table 1 that the saturation magnetization increases whereas coercivity and remenance magnetization decreases with increasing annealing temperature. The increase in annealing temperature increases the crystallite size of the samples, which results in increasing the saturation magnetization and decreasing remanance magnetization and coercivity.

The magneton number ($n_B$) was calculated by using the following relation.

$$n_B^A = \frac{M_s \times \text{Molecular weight}}{5585} \qquad \text{.............. (3)}$$

The observed values of magneton number are listed in Table 1 as a function of annealing temperature. It can be observed from table that the magneton number increases with increasing annealing temperature. Similar results of magnetic properties are reported in the literature [21, 22].

**4 Conclusions**

Cobalt ferrite nanoparticles were successfully synthesized using sol-gel auto-combustion method taking L-ascorbic acid as a fuel. The characterization of both the samples annealed at different temperature was carried out using X-ray diffraction, scanning electron microscope and which confirmed the nanocrystalline nature of the studied samples. The lattice constant, crystallite size, grain size increases with increase in annealing temperature. The saturation magnetization increases while the coercivity decreases with increase in annealing temperature. The magneton number also increases with increasing temperature.

**REFERENCES**

[1] Sh. Moradi, S. S. Madani, G. Mahmoudzadeh, M. Zhalechin, S. A. Khorrami, Int. J. Nano Dimens 3(2012)141.
[2] Choi E. J., Ahn Y., Sond K. C., J. Magn. Magn. Mater. 301 (2006)171.
[3] Noppakun Sanpo, James Wang and Christopher C. Berndt, J. Australian Ceramic Society 49(2013)84
[4] K. Maaz, S. Karim, A. Mashiatullah, J. Liu, M. D. Hou, Y. M. Sun, J. L. Duan, H. J. Yao, D. Mo, Y. F. Chen Physica B 404 (2009)3947.
[5] R. Skomski, J. Phys. Condens. Matter 15 (2003)R1.
[6] Alina Mihaela Cojocariu, Marius Soroceanu, Luminita Hrib, Valentin Nica, Ovidiu Florin Caltun, Mater. Chem. Phys. 135 (2012) 728
[7] Lawrence Kumar, Manoranjan Kar Ceri. Inter. 38 (2012) 4771.
[8] E. Veena Gopalan, I.A. Al-Omari, D. Sakthi Kumar, Yasuhiko Yoshida, P.A. Joy, M.R. Anantharaman, Appl Phys A 99 (2010) 497.
[9] Jianhong Peng, Mirabbos Hojamberdiev, Yunhua Xu, Baowei Cao, Juan Wang, Hong Wu, J. Magn. Magn. Mater. 323 (2011) 133.
[10] Y.M. Abbas, S.A. Mansour, M.H. Ibrahim, Shehab E. Ali, J. Magn. Magn. Mater. 323 (2011) 2748.
[11] M. Han, C.R. Vestal, Z.J. Zhang, J. Phys. Chem. B 108 (2004) 583.
[12] Singh P., Chalcogenide Lett., 7(2010)389.
[13] Ping Hu, De-an Pan, Xin-feng Wang, Jian-jun Tian, Jian Wang, Shen-gen Zhang, Alex A. Volinsky, J. Magn. Magn. Mater. 323 (2011)569.
[14] M.Sertkol ,Y.Koseoglu , A. Baykal , H. Kavas , M.S. Toprak J. Magn. Magn. Mater. 322(2010)866.
[15] Hong-guo Zhang, Yu-Jie Zhang, Weng-Hong Wang, Guang-Heng Wu, J. Magn. Magn. Mater. 323 (2011) 1980–1984
[16] Juliana B. Silva, Walter de Brito, Nelcy D. S. Mohallem, Mater. Sci. Engin. B 112 (2004) 182.
[17] D. V. Kurmude, C. M. Kale, P. S. Aghav, D. R. Shenngule, K. M. Jadhav J. of superc.Nov. Magn.27 (2014) 1889-1897
[18] Dao Thi Thuy Nguyet, Nguyen Phuc Duong, Le Thanh Hunga, Than Duc Hien, Takuya Satoh, J Alloys Compounds 509 (2011) 6621.
[19] N.M. Deraz, A. Alarifi, J. Anal. Appl.Pyro. 94 (2012) 41.
[20] P. Samoila, T. Slatineanu a, P. Postolache, A.R. Iordan, M.N. Palamaru Mater. Chem. Phys. 136 (2012) 241.
[21] M. M. Rashad, R. M. Mohamed. H. El-Shall, J. Mater. Pro. Tech. 198 (2008)139.
[22] Sonal Singhal, Rimi Sharma, Tsering Namgyal, Sheenu Jauhar, Santosh Bhukal, Japinder Kaur Ceri. Inter. 38 (2012) 2773.